SUPPLEMENTAL MATERIAL

Supplemental Methods

Histopathology and immunohistochemistry

Aortas were paraffin embedded and serial 5μm cross-sections were made through the length of the aorta at its largest diameter. Sections were stained with H&E (Anatech), Verhoeff's van Gieson (Sigma) for elastic lamina, Masson's trichrome (Sigma) for collagen, and Toluidine blue (Anatech) for mast cells. Elastic lamina preservation was graded as follows: grade 1, intact elastic lamina; grade 2, elastic lamina with some interruptions; and grade 3, severe elastin fragmentation. For immunohistochemistry, paraffin-embedded sections were de-waxed followed by enzymatic antigen retrieval (20μg/ml Proteinase K; Roche). Sections were Protein Blocked (Dako) and incubated separately with anti-CD3 (1:100, BD Pharmingen), anti-B220 (1:100, BD Pharmingen), anti-alpha smooth muscle actin (α-SMA, 1:200, Abcam), anti-Mac-3 (1:50, BD Pharmingen), anti-MMP2 (1:2000, Abcam) and anti-MMP9 (1:1000, Abcam) primary antibodies. Sections were incubated with the appropriate biotinylated secondary antibody (Vector Laboratories) followed by incubation with the ABC kit (Vector Lab), and visualized by 3,3'-diaminobenzidine (DAB; Vector Laboratories) and counterstained with hemotoxylin. The average number of $CD3^+$, $B220^+$, $F4/80^+$, $Mac\text{-}3^+$ and mast cells were calculated from five independent high-power fields from five sections at 50μm intervals. Some cross-sections were co-stained with fluorescent α-SMA and anti-Mac-3.

Matrix metalloproteinase activity analysis

In situ zymography and gelatin zymography were performed as previously described.[1] For *in situ* zymography, frozen optimum cutting temperature (OCT)-embedded aortic sections (10μm) from 18-day saline or AngII-infused WT and $Nf1^{+/-}$ mice were incubated with a dye-quenched gelatin substrate (DQ-gelatin, Molecular Probes) according to the manufacturer's protocol. After cleavage of DQ-gelatin by gelatinolytic activity, green fluorescence was photographed by fluorescence microscopy. Addition of EDTA (20 mM), a negative control for MMP-2 and 9 activity, in gelatin substrate was used to assess the

specificity of MMP activity. For gelatin zymography, 10 μg of homogenates lysed from segments of aorta from 18-day saline or AngII-infused WT and *Nf1*$^{+/-}$ mice were electrophoresed in a 10% SDS-polyacrylamide gel containing 1 mg/mL gelatin (Invitrogen). Gels were incubated for 36 hours in zymography buffer and stained with Coomassie brilliant blue followed by destaining to visualize bands.

***In situ* superoxide detection**

In situ dihydroethidium (DHE) staining was performed as described[2]. Cross-sections (10 μm) of OCT-embedded aortas were incubated with DHE (5 μM) (Molecular Probes Inc.) for 30 minutes and photographed using fluorescent microscopy. Mean fluorescence intensity of the digital images was quantified in the aorta at is widest point using Image J software (version 1.46, NIH).

Supplemental References

1. Satoh K, Nigro P, Matoba T, O'Dell MR, Cui Z, Shi X, Mohan A, Yan C, Abe J, Illig KA, Berk BC. Cyclophilin a enhances vascular oxidative stress and the development of angiotensin ii-induced aortic aneurysms. *Nature medicine*. 2009;15:649-656.
2. Tieu BC, Lee C, Sun H, Lejeune W, Recinos A, 3rd, Ju X, Spratt H, Guo DC, Milewicz D, Tilton RG, Brasier AR. An adventitial il-6/mcp1 amplification loop accelerates macrophage-mediated vascular inflammation leading to aortic dissection in mice. *The Journal of clinical investigation*. 2009;119:3637-3651.

Supplemental Figure 1

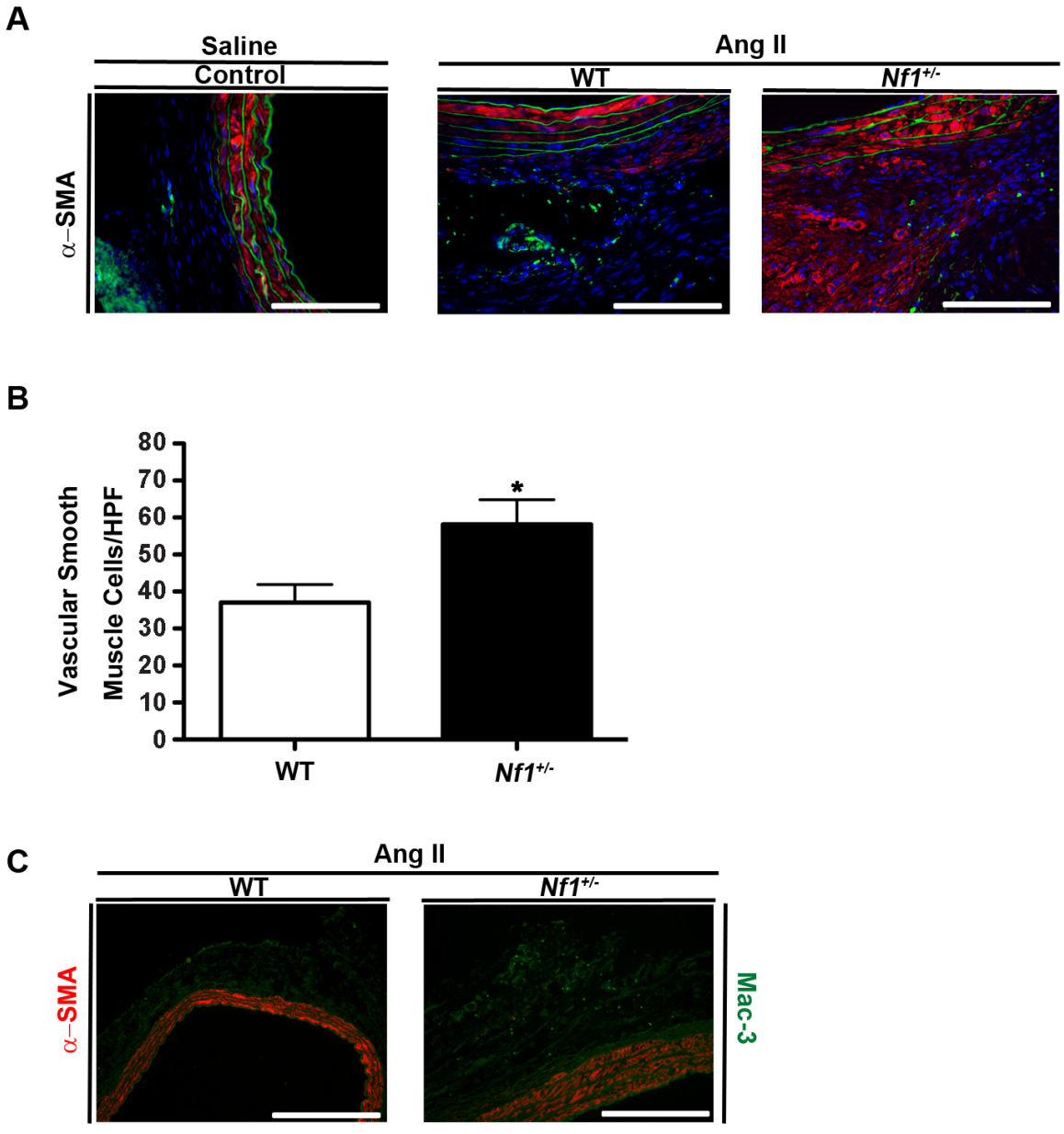

Supplemental Figure 1. AngII infusion results in increased vascular smooth muscle cell density in *Nf1*$^{+/-}$ mice. (**A**) Representative photomicrographs of abdominal aortic cross-sections from AngII-infused WT and *Nf1*$^{+/-}$ mice, stained with anti-alpha smooth muscle actin (red) to identify VSMCs. Cell nuclei are counterstained with DAPI (blue) and auto-fluorescence of murine tissue is visible (green). Saline-infused WT mice shown as control. Appearance of saline-infused *Nf1*$^{+/-}$ was similar to saline-infused WT staining. Scale bars: 50μm. (**B**) Quantification of VSMCs from AngII-infused WT (n=5) and *Nf1*$^{+/-}$ (n=5) mice; *P<0.05 for AngII-infused WT versus AngII-infused *Nf1*$^{+/-}$, by Student's t-test. (**C**) Representative photomicrographs showing co-staining of AngII-infused WT and *Nf1*$^{+/-}$ aortas with anti-α-SMA (red) and anti-Mac-3 (green). Scale bars: 50μm

Supplemental Figure 2

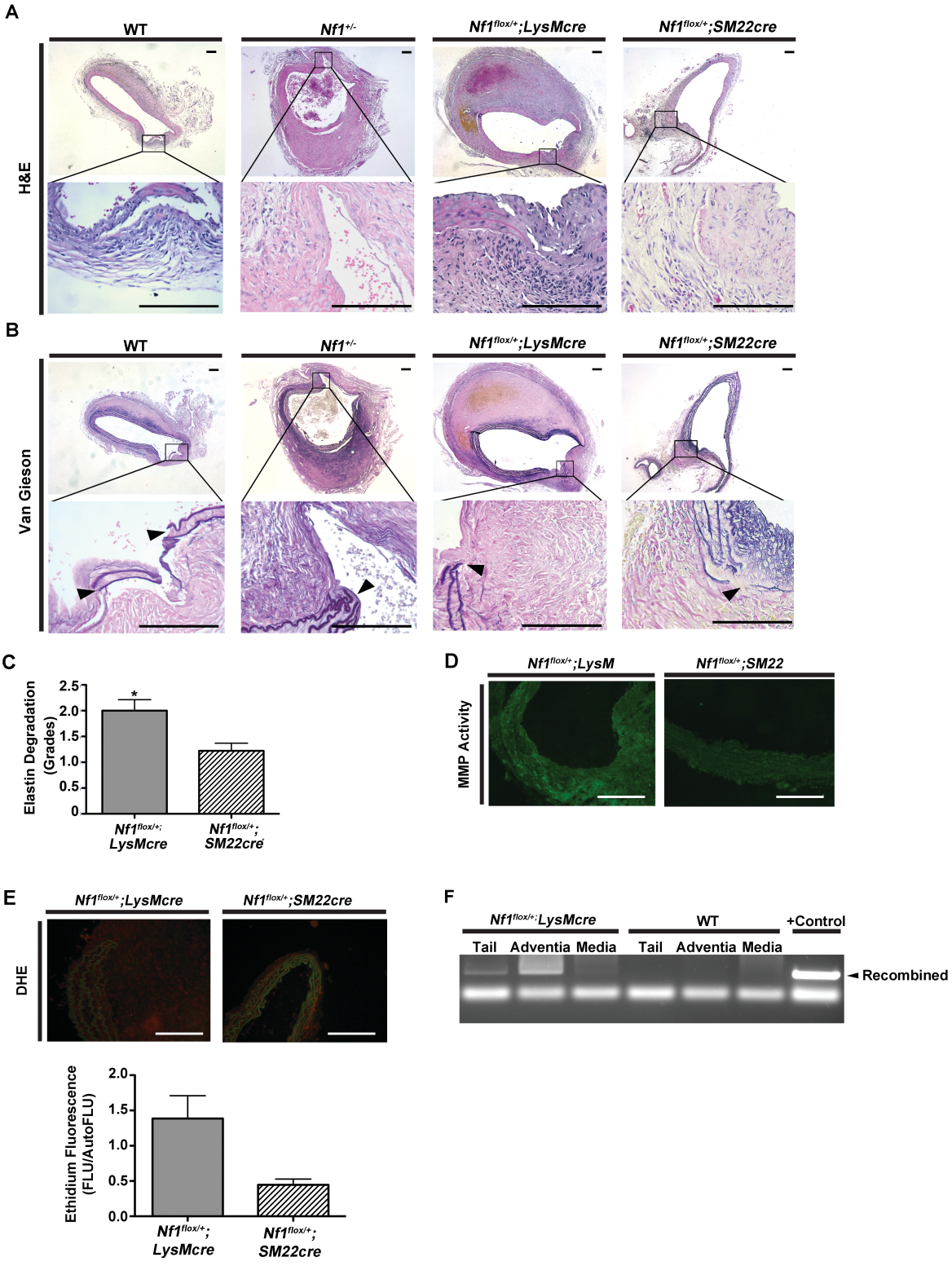

Supplemental Figure 2. *Cre*-mediated ablation of a single *Nf1* allele in myeloid cells alone recapitulates AAA formation in *Nf1*$^{+/-}$ mice. (**A**) Representative photomicrographs of abdominal aortic cross-sections from AngII-infused WT, *Nf1*$^{+/-}$, *Nf1*$^{flox/+}$*;LysMcre* and *Nf1*$^{flox/+}$*;SM22cre*, stained with H&E or (**B**) van Gieson for elastin. Boxes identify area that is magnified in lower panel. Arrowheads identify fragmentation of elastic lamina in van Gieson photomicrographs and yellow staining identifies extracellular matrix. Saline infusion did not produce aneurysms in any genotype (data not shown). Scale bars: 50μm. (**C**) Grading of elastic lamina degradation in AngII-infused *Nf1*$^{flox/+}$*;LysMcre* and *Nf1*$^{flox/+}$*;SM22cre* mice. **P*<0.05 for *Nf1*$^{flox/+}$*;LysMcre* (*n*=12) versus *Nf1*$^{flox/+}$*;SM22cre* (*n*=9). No statistical significance in elastic lamina degradation grade was observed between *Nf1*$^{flox/+}$*;LysMcre* and *Nf1*$^{+/-}$ mice or *Nf1*$^{flox/+}$*;SM22cre* and WT mice (data not shown). (**D**) Representative photomicrographs showing MMP activity in *Nf1*$^{flox/+}$*;LysMcre* and *Nf1*$^{flox/+}$*;SM22cre* mice. Scale bars: 50μm. (**E**) Representative photomicrographs of abdominal aortic cross-sections from saline or AngII-infused WT and *Nf1*$^{+/-}$ mice, showing superoxide production identified by *in situ* DHE staining (red). Auto-fluorescence of murine tissue is visible (green). Scale bars: 50μm. Bar graph depicts quantification of ethidium fluorescence. (**F**) PCR analysis of abdominal aorta shows the specific location of the *cre*-mediated recombination of floxed *Nf1* gene in the vascular adventitia of 3 month old, non-infused *Nf1*$^{flox/+}$*;LysMcre* mice. Arrowhead indicates cre-mediated recombination (280bp band). *Nf1*$^{flox/+}$*;SM22cre* VSMCs were used as positive control.

Supplemental Figure 3

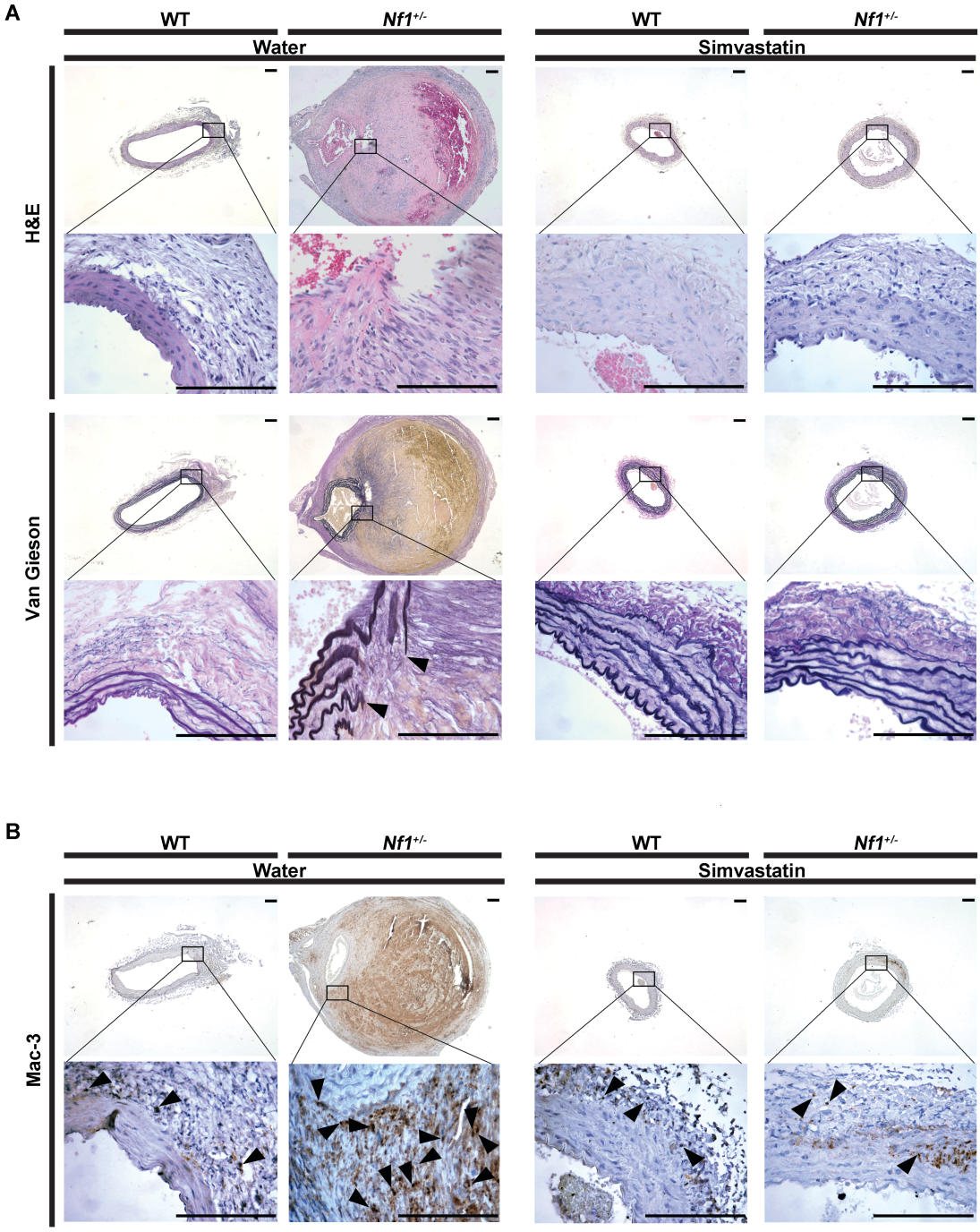

Supplemental Figure 3. Simvastatin prevents AngII-induced AAA formation in *Nf1*$^{+/-}$ mice. (**A**) Representative photomicrographs of abdominal aortic cross-sections from water or simvastatin-treated, AngII-infused WT and *Nf1*$^{+/-}$ mice stained with H&E, van Gieson for elastin or (**B**) anti-Mac-3 (arrowheads). Boxes specify area magnified in lower panel. Saline-infused WT and *Nf1*$^{+/-}$ mice treated with water or simvastatin did not produce aneurysms (data not shown). In **A**, arrowheads identify fragmentation of elastic lamina and yellow staining identifies extracellular matrix. Scale bars: 50μm.

Supplemental Figure 4

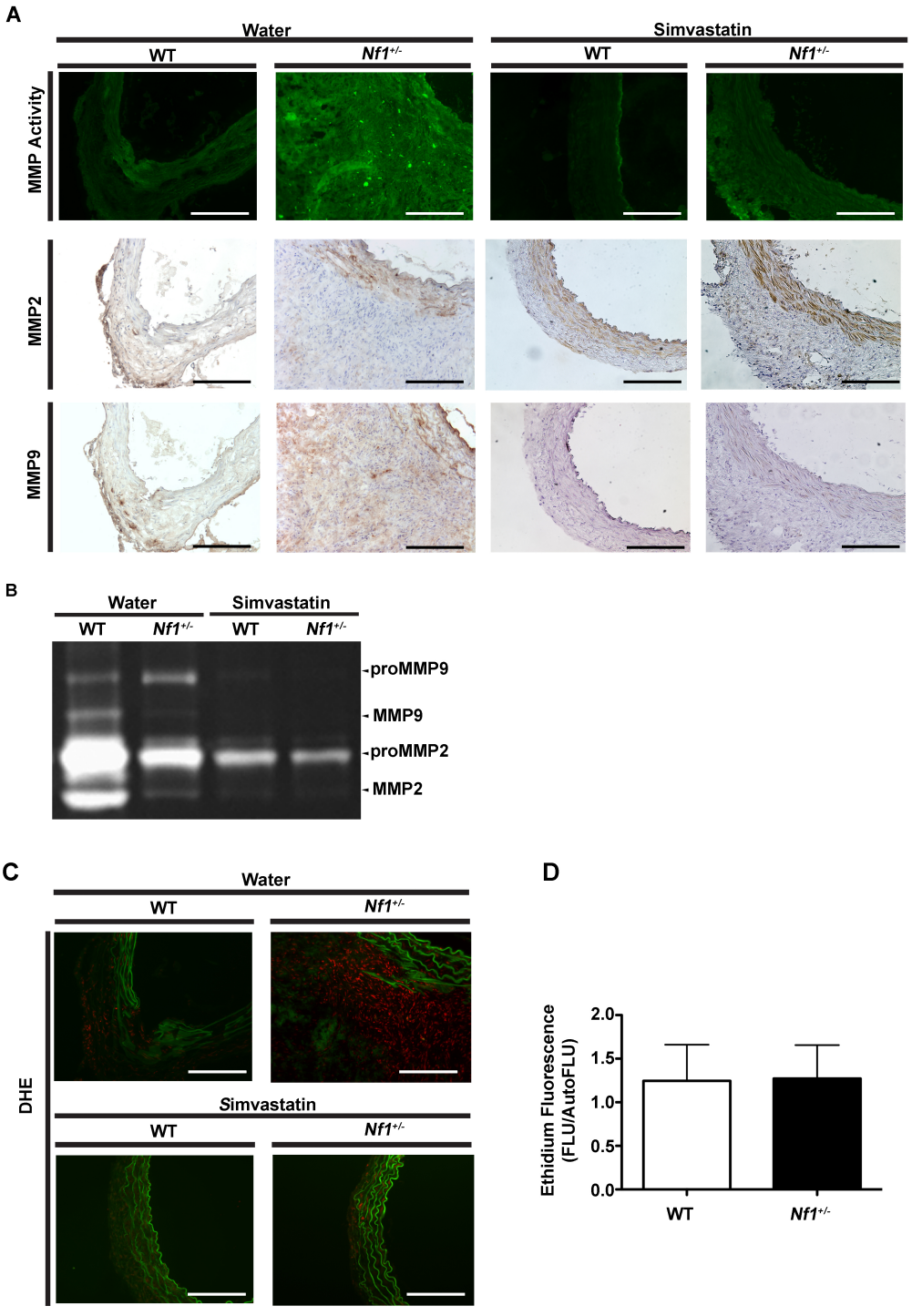

Supplemental Figure 4. Simvastatin attenuates MMP expression and activation and ROS production induced by AngII in *Nf1*$^{+/-}$ mice. (**A**) Representative photomicrographs of abdominal aortic cross-sections from water or simvastatin treated, AngII-infused WT and *Nf1*$^{+/-}$ mice. MMP activity (green) was visualized by *in situ* zymography and expression of MMP-2 and MMP-9 was detected by immunohistochemical staining with anti-MMP-2 (brown) and anti-MMP-9 antibodies (brown). Scale bars, 50μm. (**B**) Representative zymogram showing abdominal aortic MMP-2 and MMP-9 levels from water or simvastatin treated, AngII-infused WT and *Nf1*$^{+/-}$ mice. (**C**) Representative photomicrographs of abdominal aortic cross-sections from water or simvastatin treated, AngII-infused WT and *Nf1*$^{+/-}$ mice showing ROS identified by *in situ* DHE staining (red). Autofluorescence of murine tissue is visible (green). (**D**) Quantification of ethidium fluorescence for simvastatin-treated, AngII-infused WT and *Nf1*$^{+/-}$.

Supplemental Figure 5

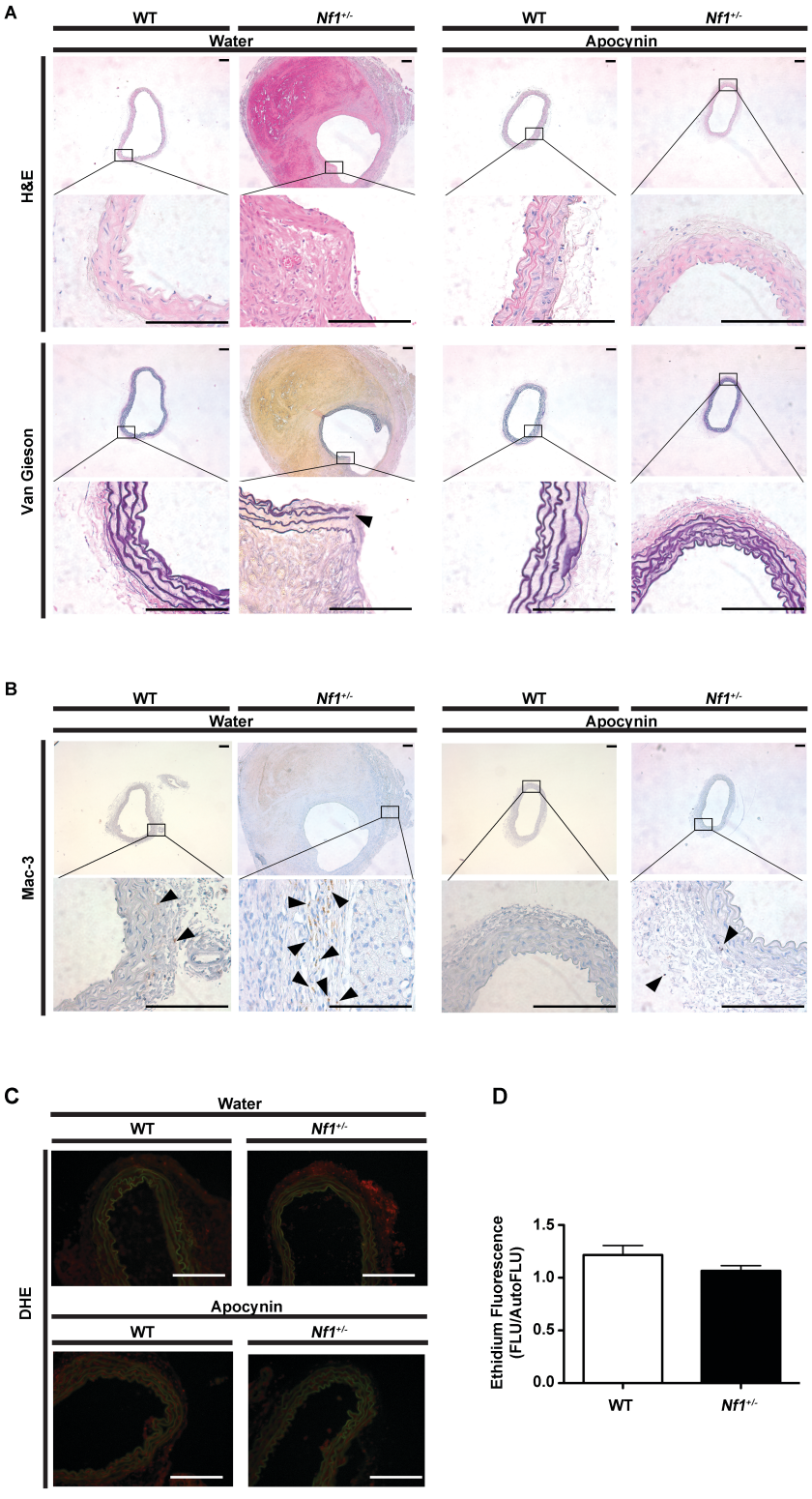

Supplemental Figure 5. Apocynin prevents AngII-induced AAA formation in *Nf1*$^{+/-}$ mice. (**A**) Representative photomicrographs of abdominal aortic cross-sections from water or apocynin-treated, AngII-infused WT and *Nf1*$^{+/-}$ mice stained with H&E, van Gieson for elastin or (**B**) anti-Mac-3 (arrowheads). Boxes specify area magnified in lower panel. Saline-infused WT and *Nf1*$^{+/-}$ mice treated with water or apocynin did not produce aneurysms (data not shown). In **A**, arrowhead identifies fragmentation of elastic lamina and yellow staining identifies extracellular matrix. Scale bars: 50μm. (**C**) Representative photomicrographs of abdominal aortic cross-sections from water or apocynin treated, AngII-infused WT and *Nf1*$^{+/-}$ mice showing ROS identified by *in situ* DHE staining (red). Auto-fluorescence of murine tissue is visible (green). (**D**) Quantification of ethidium fluorescence for apocynin-treated, AngII-infused WT and *Nf1*$^{+/-}$.